

Long-Range Correlation Length and Isothermal Compressibility of Carbon Dioxide Near the Critical Point

Joseph H. Lunacek and David S. Cannell

Department of Physics, University of California, Santa Barbara, California 93106

(Received 6 July 1971)

We have measured the angular dependence and total intensity of light scattered by carbon dioxide near its critical point, shown that the Ornstein-Zernike theory is inadequate, and determined the temperature dependence of the isothermal compressibility κ_T and the long-range correlation length ξ . The exponents describing the divergences of κ_T and ξ above the critical temperature are $\gamma = 1.219 \pm 0.01$ and $\nu = 0.633 \pm 0.01$, respectively. The exponent describing the departure from the Ornstein-Zernike theory is $\eta = 0.074 \pm 0.035$.

It has been predicted by Ornstein and Zernike (OZ),¹ and verified experimentally,² that the angular distribution of the intensity of light scattered by a pure fluid near its critical point is accurately given by

$$I(\vec{K}) = A\kappa_T \sin^2\varphi / (1 + K^2\xi^2), \quad (1)$$

where κ_T is the isothermal compressibility, A is a constant which can be evaluated at any temperature, φ is the angle between the electric field of the incident light and the scattered wave vector; and K is the scattering wave vector $2k_0 \sin\frac{1}{2}\theta$, where k_0 is the wave vector of the incident light in the fluid and θ is the scattering angle. The above expression defines the OZ correlation length ξ . As the critical point is approached, ξ and κ_T diverge as $(T - T_c)^{-\nu}$ and $(T - T_c)^{-\gamma}$, respectively. The fluctuation theorem for the isothermal compressibility together with the OZ form of the correlation function yields the result $2\nu = \gamma$. Both ξ and κ_T can be determined independently by measuring the asymmetry and total intensity of light scattered by the fluid, thus offering an ideal method of checking the theory. In addition, measurements of ξ can be used to check predictions³ concerning the dynamic behavior of critical fluids.

We have made accurate measurements of the differences in and magnitudes of the intensity of light scattered through the angles $\theta_F = 17.5^\circ$ and $\theta_B = 168.5^\circ$ in carbon dioxide. The measurements were made on the critical isochore over the temperature range $0.023 \leq T - T_c \leq 10.00^\circ\text{C}$. We also measured the total scattered intensity over essentially the same range. Since the anisotropy becomes very small at higher temperatures,² the measurements were made using a differential technique with the apparatus shown in Fig. 1.

The scattering cell was constructed of berylli-

um copper, optical glass, and indium. Its temperature was controlled to $\pm 0.001^\circ\text{C}$, and measured using a platinum resistance thermometer. It was filled to within 0.1% of the critical density with carbon dioxide containing less than 50 ppm of impurities. The density was determined by measuring the meniscus height as a function of temperature using the data of Michels, Blaisse, and Michels⁴ for the shape of the coexistence curve. This also determined the critical temperature, and yielded the value $31.000 \pm 0.001^\circ\text{C}$, which coincided with the temperature of meniscus disappearance. A differential scattered-intensity measurement was made by removing the beam splitter and blocking the transmitted beam. Light scattered through the angle θ_F was collected using the optics L_1 , L_2 , and L_3 . The variable aperture A determined the collection solid angle. Lenses L_1 and L_2 imaged the scattering region on the slit S , thus determining that section of the beam from which scattering was accepted. The optics for θ_B functioned identically. Lenses L_3 and L_3' focused the light from each channel

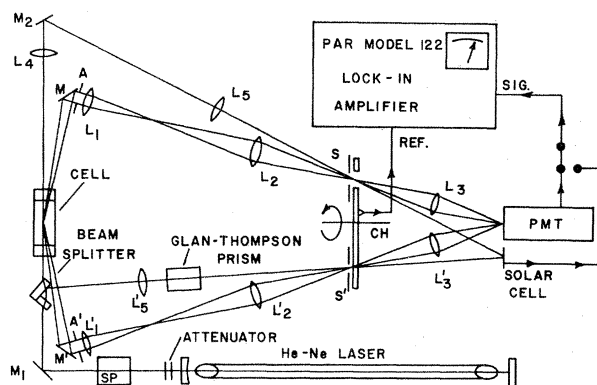


FIG. 1. Schematic diagram of the apparatus.

onto the same spot on the photocathode of an RCA 7265 photomultiplier. The chopper *CH* alternately accepted light from each channel. The photocurrent was passed to a lock-in amplifier whose reference was generated by the chopper. Its output was proportional to the difference in the intensity of the light collected by each channel. The intensity collected by either channel alone was measured by blocking the other channel.

To measure the total scattered intensity, the attenuation of the beam by the fluid was determined by comparing the reference and transmitted beams.⁵ The beams passed through the chopper and fell on a solar cell whose output went to the lock-in. The Glan-Thompson prism served as a variable attenuator.

In making either differential or total scattered-intensity measurements, the lock-in output can be written as $V = G_F I_F - G_B I_B$. For a differential scattered-intensity measurement, I_F and I_B are the scattered powers per unit solid angle for the angles θ_F and θ_B , and the gains G_F and G_B are determined by the collection solid angles; lens, window, and mirror losses; photomultiplier gain; and electronic gains. For a total scattered-intensity measurement, I_B and I_F are the respective intensities of the incident and transmitted beams *in the cell*. The gains are determined by the beam splitter, Glan-Thompson setting, etc.

We now consider the differential scattered intensity. For each temperature T_i the ratio of the lock-in output with both channels open to that with only the forward channel open is

$$S_\xi(T_i) = 1 - \frac{G_B I_B}{G_F I_F} \equiv 1 - \frac{G_B f_\xi(T_i)}{G_F}, \quad (2)$$

where $f_\xi(T_i) = [1 + K_F^2 \xi^2(T_i)] / [1 + K_B^2 \xi^2(T_i)]$ with K_F and K_B the scattering wave vectors for the angles θ_F and θ_B . For each pair of temperatures the ratio

$$R_{ij}^\xi \equiv \frac{1 - S(T_i)}{1 - S(T_j)} = \frac{f_\xi(T_i)}{f_\xi(T_j)} \quad (3)$$

was computed. Thus the measurements determine the ratios $f_\xi(T_i)/f_\xi(T_j)$. If ξ is assumed to have the form $\xi_0 [(T - T_c)/T_c]^{-\nu}$, then ξ_0 and ν can be determined. The best fit for ξ was used to calculate G_B/G_F by using Eq. (2) with data points at $T - T_c = 4.420^\circ\text{C}$. The correlation range for all other points was calculated with this value for G_B/G_F . The points and the best fit to ξ are shown in Fig. 2.

A similar procedure was utilized in interpreting the total scattered-intensity measurements.

In this case the $S_\tau(T_i)$ to be used is

$$S_\tau(T_i) = 1 - \frac{G_F I_F}{G_B I_B} \equiv 1 - \frac{G_F}{G_B} \exp[-\tau(T_i)L], \quad (4)$$

where $\tau(T_i)$ is the attenuation per unit length in the fluid, L is the path length in the cell, and I_B and I_F are the intensities of the incident and transmitted beam *in the cell*. The transmission and reflectivity of the beam splitter and the cell-window losses are included in the gains. The experimentally determined ratios thus take the form

$$R_{ij}^\tau \equiv \frac{1 - S_\tau(T_i)}{1 - S_\tau(T_j)} = \exp[\{\tau(T_j) - \tau(T_i)\}L], \quad (5)$$

providing the difference in the attenuation for any two temperatures. The attenuation τ may be related to κ_T by integrating Eq. (1) over angles, yielding⁵

$$\tau = \pi A \kappa_T \times \left[\frac{(2\alpha^2 + 2\alpha + 1)}{\alpha^3} \ln(1 + 2\alpha) - \frac{2(1 + \alpha)}{\alpha^2} \right], \quad (6)$$

where $\alpha = 2k_0^2 \xi^2$; $A = (\pi^2 k_B T / \lambda_0^4) (\rho \partial \epsilon / \partial \rho)_T^2$, where λ_0 is the vacuum wavelength of the light, k_B is Boltzmann's constant, T is the absolute temperature, ρ is the density, and ϵ is the dielectric constant. The quantity $(\rho \partial \epsilon / \partial \rho)_T^2 = [(n^2 - 1)(n^2 + 2)]^2 / 9$ was calculated by using the Lorentz-Lorenz relation and measured values of the index of refraction⁷ n . If κ_T is assumed to have the form $\kappa_0 [(T$

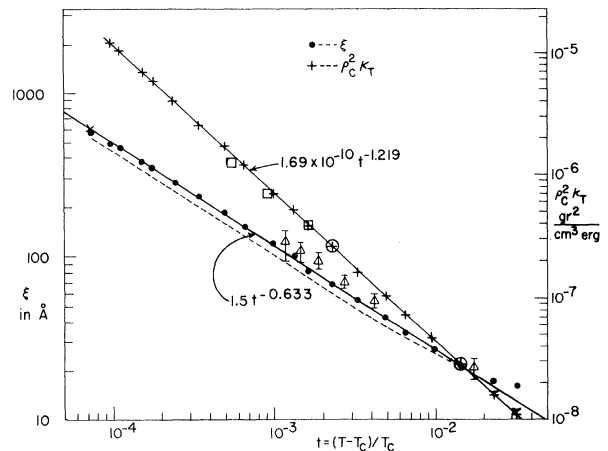


FIG. 2. The long-range correlation length and susceptibility $\rho_c^2 \kappa_T$ of carbon dioxide along the critical isochore as a function of the reduced temperature $t = (T - T_c)/T_c$. The triangles are x-ray scattering results from Ref. 6. The squares are from the static PVT data of Ref. 4. The circles are our own determination of the absolute compressibility.

$-(T_c)/T_c]^{-\gamma}$ then κ_0 and γ can be determined. Figure 2 shows the fit and the experimental values for the isothermal compressibility, presented as $\rho_c^2 \kappa_T$. The points were obtained in the same manner as those for ξ . We also determined the compressibility absolutely by measuring the ratio of the forward scattered intensity at two temperatures. As seen from Eq. (1) this determines the ratio of the compressibilities at those temperatures. A different relationship involving the compressibility is obtained from R_{ij}^T which gives the difference in the attenuation τ for the two temperatures. In computing the ratio we were able to eliminate the effect of attenuation by the fluid, using our value for the difference in τ at those two temperatures. By using Eq. (6) and the measured values for ξ , this difference may be combined with the ratio of the compressibilities to yield the compressibility at those two temperatures. These values are shown as open circles in Fig. 2. The analysis yields the following results for ξ and κ_T :

$$\xi = (1.50 \pm 0.09) [(T - T_c)/T_c]^{-0.633 \pm 0.01} \text{ \AA},$$

$$\kappa_T = (7.75 \pm 0.46) \times 10^{-10}$$

$$\times [(T - T_c)/T_c]^{-1.219 \pm 0.01} \text{ cm}^2/\text{dyn}.$$

The errors were obtained by varying one parameter while adjusting the other in order to maintain a best fit, until the rms deviation of the fit from the points was twice that of the best fit.

The OZ expression for the angular dependence of the scattered intensity accurately represents our data with the above power-law dependences for ξ and κ_T . However, the theory also predicts that $2\nu = \gamma$, which disagrees with our results. We conclude that the OZ theory is inadequate to describe completely the long-range correlation near the critical point. This failure has been anticipated theoretically and modifications have been worked out.⁸ The principal modification is the introduction of an exponent η describing the departure of the angular dependence from that of Eq. (1). The exponent relationship becomes $(2 - \eta)\nu = \gamma$, which with our values for ν and γ yields $\eta = 0.074 \pm 0.035$. We also analyzed our data using the modified theory and this value of η , but no significant change occurred either in the fits or in ν or γ .

Recently, Kawasaki³ has derived an expression for the critical part Γ_c of the Rayleigh linewidth $\Gamma_R = \Lambda K^2/\rho_0 C_p$ of a pure fluid near its critical

point, namely,

$$\Gamma_c = \frac{k_B T}{8\pi\eta_s \xi^3} \left\{ 1 + (K\xi)^2 + \left[(K\xi)^3 - \frac{1}{K\xi} \right] \tan^{-1} K\xi \right\}, \quad (7)$$

where η_s is the shear viscosity. The derivation used the OZ correlation function, but for our range of $K\xi$ it is very insensitive to $\eta \leq 0.1$. By using measured values for the thermal conductivity⁹ Λ , it is possible to obtain values for Γ_c from the measured values¹⁰ Γ_R . Since η_s is known,¹¹ our measurements of ξ provide the means of checking Eq. (7). We have done so by using the measured values of Γ_c and the $K=0$ limit of Eq. (7) to compute ξ in the temperature range $0.023 \leq T - T_c \leq 4.0^\circ\text{C}$. The values of ξ obtained in this manner are shown as the dashed line in Fig. 2, where they may be compared with our measured values. The agreement is within the error for the linewidths and corrections.

The stability was enhanced by mounting the system on a massive table and by temperature controlling the photomultiplier. The value of the difference in the scattered intensities at any temperature was reproducible to within $\pm 0.05\%$ of the scattered intensity. The error caused by stray light increases as $T - T_c$ is increased because of the reduction in the scattered intensity. We estimated its effect by extending our measurements to $T - T_c = 17.8^\circ\text{C}$, and attributing all of the difference between the measured asymmetry and the value obtained by extrapolating our fit to stray light. The one-sided error bars on the two highest temperature points in Fig. 2 represent the possible effect of stray light. At $T - T_c = 4.42^\circ\text{C}$ the stray light contributed less than 0.03% to the asymmetry of 0.23% . The extremely low stray-light level was achieved by orienting the cell so that the background viewed by either set of optics was a cell window viewed in a plane containing no specular reflections. For temperatures near T_c , the primary difficulty arises from multiple scattering. At $T - T_c = 0.023^\circ\text{C}$ we estimated its effect by observing the asymmetry and intensity of the multiple scattering occurring immediately above the beam. Correcting for this effect moves the point at $T - T_c = 0.023^\circ\text{C}$ in Fig. 2 to the point indicated by the X. To eliminate heating by the beam we attenuated it until the results were independent of beam power. An error present at all temperatures arises from the attenuation of light by the fluid. It arises if the path length in the cell differs for the two channels. For our geometry this effect changes all the values of ξ by essentially the same percent-

age, the maximum difference in the changes being less than 0.5% and the changes being less than 4%.

In conclusion, our measurements of the long-range correlation length and isothermal compressibility of CO₂ indicate that the Ornstein-Zernike theory is inadequate to describe completely the form of the long-range correlation function in a pure fluid near its critical point. Our measurements together with the exponent relation $(2 - \eta)\nu = \gamma$ lead to the result that $\eta = 0.074 \pm 0.035$. In addition, our measurements, together with measurements of the thermal conductivity,⁹ Rayleigh linewidth,¹⁰ and shear viscosity,¹¹ show that the critical part of the Rayleigh linewidth is adequately described by the dynamical theory due to Kawasaki.³ We should mention that White and Maccabee¹² have recently measured κ_T for CO₂, obtaining $\gamma = 1.17 \pm 0.02$ which disagrees with our result.

The authors wish to thank Professor Richard A. Ferrell for many valuable suggestions. We also acknowledge with thanks stimulating conversations with Dr. Marzio Giglio, and wish to extend special thanks to Professor Stuart B. Dubin who aided us immeasurably in the original design and testing of the apparatus. We also wish to

thank Professor George B. Benedek for providing us with the temperature controller used in the experiment. We were aided immeasurably in our efforts by the skill and meticulous craftsmanship of Mr. Hans R. Stuber.

¹L. S. Ornstein and F. Zernike, Proc. Acad. Sci. Amsterdam 17, 793 (1914), and Phys. Z. 19, 134 (1918).

²M. Giglio and G. B. Benedek, Phys. Rev. Lett. 23, 1145 (1969).

³K. Kawasaki, Phys. Rev. A 1, 1750 (1970).

⁴A. Michels, B. Blaisse, and C. Michels, Proc. Roy. Soc., Ser. A 160, 358 (1937).

⁵V. G. Puglielli and N. C. Ford, Jr., Phys. Rev. Lett. 25, 143 (1970).

⁶B. Chu, J. S. Lin, and J. A. Duisman, Phys. Lett. 32A, 95 (1970).

⁷J. Straub, Ph. D. thesis, Technische Hochschule, München, 1965 (unpublished).

⁸M. E. Fisher, J. Math. Phys. 5, 944 (1964).

⁹J. V. Sengers and P. H. Keyes, Phys. Rev. Lett. 26, 70 (1971).

¹⁰H. L. Swinney and H. Z. Cummins, Phys. Rev. 171, 152 (1968).

¹¹J. Kestin, J. H. Whitelaw, and T. F. Zien, Physica (Utrecht) 30, 16 (1964).

¹²J. A. White and B. S. Maccabee, Phys. Rev. Lett. 26, 1468 (1971).

Time Correlations of X-Ray Spectra with Neutron Emission from a Plasma-Focus Discharge

M. J. Bernstein, C. M. Lee,* and F. Hai

Plasma Research Laboratory, The Aerospace Corporation, El Segundo, California 90045
(Received 11 March 1971)

Time correlations between neutron and x-ray emissions from a plasma-focus discharge are strongly dependent on photon energy. The time history of neutron emission coincides with that of nonthermal x-ray emission above 30 keV, in a manner consistent with an acceleration model for neutron production. Plasma x radiation below 5 keV corresponds to $T_e = 0.4$ keV and does not correlate with neutron emission.

Plasma-focus discharges generate intense neutron pulses (up to 10^{18} D-D neutrons/sec) by means of a mechanism which is not yet well understood. The characteristics of both the neutron emission and the accompanying radiation have been the subject of many investigations, but there are large inconsistencies in the results and interpretations, particularly with regard to correlations between neutron and x-ray emission.¹⁻⁵ Values cited for the electron temperature T_e range from 0.5 to 10 keV,^{1,2,4,6,7} while other time-integrated measurements have revealed

that the x-ray spectra over a broad range (6-300 keV) does not correspond to thermal radiation.^{8,9} To resolve such discrepancies, we have made time-resolved measurements of the emitted radiation over a wide spectral range (1-200 keV) using suitable spectral resolution. This x-ray emission was correlated in time with the rate of D-D neutron emission and also with streak photographs of the visible plasma diameter. The results explain many contradictions in the previously reported characteristics and provide strong evidence that the neutron production is associat-